Published in final edited form as:
Rapid Commun Mass Spectrom. 2009 February ; 23(3): 409–418. doi:10.1002/rcm.3894.

Transmission Mode Ion/Ion Reactions in the RF-only Ion Guide of Hybrid Tandem Mass Spectrometers

Joshua F. Emory[†], **Kerry H. Hassell**[†], **Frank A. Londry**[‡], and **Scott A. McLuckey**[†,*]
[†]Department of Chemistry, Purdue University, West Lafayette, IN 47907-2084, USA

[‡]MDS SCIEX, 71 Four Valley Drive, Concord, Ontario, Canada L4K4V8

Abstract

Transmission mode ion/ion reactions have been performed within the first quadrupole, the Q0 RF-only quadrupole, of two types of hybrid tandem mass spectrometers (viz., triple quadrupole/linear ion trap and QqTOF instruments). These transmission mode reactions involved the storage of either the reagent species and the transmission of the analyte species through the Q0 quadrupole for charge inversion reactions or the storage of the analyte ions and transmission of the reagent ions as in charge reduction experiments. A key advantage to the use of transmission mode ion/ion reactions is that they do not require any instrument hardware modifications to provide interactions of oppositely charged ions and can be implemented in any instrument that contains a quadrupole or linear ion trap. The focus of this work was to investigate the potential of using the RF-only quadrupole ion guide positioned prior to the first mass-resolving element in a tandem mass spectrometer for ion/ion reactions. Two types of exemplary experiments have been demonstrated. One involved a charge inversion reaction and the other involved a charge reduction reaction in conjunction with ion parking. Ion/ion reactions proved to be readily implemented in Q0 thereby adding significantly greater experimental flexibility in the use of ion/ion reaction experiments with hybrid tandem mass spectrometers.

Keywords

Ion/ion reactions; hybrid tandem mass spectrometer; charge inversion; RF-only quadrupole

INTRODUCTION

Ion/ion reactions have proved to be particularly useful in altering the charge states of ions formed via electrospray ionization (ESI)1 by using primarily proton transfer chemistry2,3,4,5,6,7 to reduce the charges of macro-ions in the gas-phase. The high exothermicities and large reaction cross-sections8 of ion/ion reactions make them particularly effective in manipulating charge states of ions in the gas phase. Ion/ion reactions have proven especially useful in the simplification of spectra derived from the ESI of polymer mixtures6,7,8, 9, and product ion spectra obtained from multiply charged ions within ion traps10, 11,12,13,. In addition, ion/ion reactions have been used to simultaneously concentrate and charge-state purify a protein ion in the gas phase using a technique referred to as ion parking14,15. Multiple proton transfers within a single ion/ion reaction encounter can also be used to invert the polarity of an ion in the gas phase16, 17. An advantage of inverting the polarity of an ion in the gas phase is that it separates the ionization polarity from the analysis polarity. This allows the analyte to be ionized in most

*Phone: (765) 494-5270, Fax: (765) 494-0239, E-mail: mcluckey@purdue.edu.

efficient ionization polarity and then analyzed in the opposite polarity to obtain additional structural information. An example of this type of experiment involved the charge inversion of a phosphopeptide anion to form a doubly charged cation, which was subsequently dissociated by electron transfer dissociation (ETD) for the localization of the phosphorylation site18.

Ion/ion reactions in tandem mass spectrometry were first developed and implemented on 3D quadrupole ion trap4,19. Recently, 2D linear ion traps20,21 (LITs) have also been adapted for ion/ion reactions22,23. In some cases, the LIT has been a component of a hybrid instrument, which combine elements of ion trapping with ion transmission based devices, such as mass filters23, and/or with other mass analyzers such as time of flight (TOF)24, ion cyclotron resonance25, and OrbitrapTM, 26,27 instruments. Most ion/ion reactions are performed in mutual storage mode, where both ion polarities are stored simultaneously in overlapping regions of space. In 3D ion traps, the radio frequency (RF) trapping field operates in three-dimensions, which enables the storage of oppositely charged ions without the need for any modification of the ion trap. Mutual storage of oppositely charged ions in 2D LITs, however, requires means for the storage of oppositely charged ions in the axial dimension, for which a radio-frequency trapping field is ordinarily absent. The application of auxiliary RF voltages to the containment lenses of the LIT22 or operation of the quadrupole array in an unbalanced condition28 is therefore commonly performed to enable mutual storage of oppositely charged ions in 2D LITs.

Ion/ion reactions can also be implemented in LITs by storing one of the reactant ion populations using static trapping potentials on the containment lenses while the other reactant ion population is transmitted through the quadrupole array29,30. This approach, which has been referred to as “transmission mode”, does not require the application of auxiliary RF to the end lenses of the LIT or operation of the quadrupole array in an unbalanced condition and avoids the need for a distinct mutual ion storage period, which can result in an improved duty cycle relative to a mutual storage mode experiment.

In principle, any quadrupole array can be used for transmission mode ion/ion reactions provided that the pressures within the quadrupole array are high enough to trap ions efficiently and provide good spatial overlap of the oppositely charged ions and that effective DC trapping potentials can be applied to the end lenses of the quadrupole array. Electrodynamic multi-pole devices are frequently used to transfer ions from the relatively high pressure region of an ESI atmosphere/vacuum interface to lower pressure regions of the instrument. In the case of many hybrid triple quadrupole/LIT and QqTOF instruments, a quadrupole array, referred to as Q0, performs this function by transmitting ions that issue from the interface region to a mass resolving quadrupole, referred to as Q1. The pressure in Q0 is typically on the order of 10 mTorr N_2, which is used as the curtain gas in the ESI interface. The ability to perform ion/ion reactions in Q0 provides enhanced experimental flexibility in hybrid instruments because they allow for an ion processing step to take place prior to ions passing through the mass resolving quadrupole (Q1) and the subsequent analysis steps. We demonstrate here proton transfer charge inversion and charge reduction reactions within the Q0 quadrupoles of hybrid triple quadrupole/LIT and QqTOF platforms and provide illustrative examples of the use of ion/ion reactions in both Q0 and Q2 in a single experiment.

EXPERIMENTAL

Materials

Charge inversion reagent solutions of polypropylenimine diamino-butane (DAB) and polyamidoamine (PAMAM) dendrimers were made in aqueous ~1–2% acetic acid and in

aqueous ~1–2% ammonium hydroxide, respectively, to achieve final concentrations of ~1 mg/mL. For charge reduction experiments, pentadeca-fluoro-1-octanol (PFO) was prepared in a ~0.4 mg/mL solution of 49/49/2 (v/v/v) methanol, water, ammonium hydroxide. Peptide solutions for the charge inversion experiments were made in an aqueous solution of ~10 μM of peptide dissolved in 49.5/49.5/1 (v/v/v) methanol/water, with ~1% ammonium hydroxide (negative ion formation) or acetic acid (positive ion formation). Protein solutions for ion parking experiments were prepared at concentrations of 10–20 μM of each protein component dissolved in (49/49/2) water/methanol/acetic acid. All reagents (dendrimers and PFO) and all analytes (peptides and proteins) were obtained from Sigma Aldrich (St. Louis, MO, USA).

Instrumentation

Experiments were performed using one of three modified instruments from Applied Biosystems/MDS Sciex, Concord, ON, Canada. These instruments were a QTRAP 2000, QTRAP 4000, and a QSTAR XL, which had been modified to allow for ion/ion reactions[24, 31, 32]. In all three instruments, two nano-ESI emitters, which were operated in a pulsed mode (see below), were positioned before the atmosphere/vacuum interface to allow for the formation and admission of the analyte and reagent ions. The QTRAP instruments are both hybrid triple quadrupole/LIT instruments and the QSTAR XL is a quadrupole/time-of-flight instrument. Each QTRAP is comprised of four co-linear quadrupole arrays, Q0-Q3 while the QSTAR XL is comprised of three collinear quadrupole arrays, Q0-Q2, coupled to an orthogonal acceleration reflectron-TOF mass analyzer. The Q0 arrays in all of the instruments have been modified to allow for the superposition of a supplementary low RF voltage to a pair of opposing rods to enable the resonance excitation of ions within the array. The 4000 QTRAP was controlled by a research version of MS Expo software version 3.7 provided by MDS Sciex, and all electronics on the 2000 QTRAP and QSTAR XL instruments were controlled by Daetalyst 3.14, a research version of software also provided by MDS Sciex. Ion ejection in the 2000 and 4000 QTRAP instruments was performed by subjecting the ions to mass-selective axial ejection[33] (MSAE) using a supplementary RF signal at a frequency of 310 kHz for the 2000 QTRAP and 810 kHz for the 4000 QTRAP to eject the ions from the Q3 cell. The spectra obtained from the QTRAPs are typically the averages of ~20 individual scans, and the spectra obtained from the QSTAR XL are an average of ~10 scans except for the CID spectrum, which is an average of 3000 scans.

Transmission Mode Charge Inversion Reaction Sequence

For transmission mode negative-to-positive charge inversion reaction experiments in Q0 of a QTRAP, the positive high-voltage power supply for the nanospray source was pulsed on to generate DAB dendrimer cations, which were admitted into the Q0 quadrupole and stored there by the application of a repelling +22 V DC to a lens situated between Q0 and Q1. The DAB dendrimer ions were cooled in Q0 at a pressure of ~10 mTorr of nitrogen for 50 ms, while the high voltage on the positive nanospray was turned off and the DC potentials applied to the curtain plate and orifice were adjusted to allow ions of the opposite polarity (the analyte ion) to enter Q0. After the cooling step, the power supply connected to the negative nanospray emitter was triggered on to generate negative peptide ions, which were transmitted through the Q0 quadrupole where they could react with the dendrimer ions. After the transmission of analyte ions through the Q0 quadrupole, a second ~50 ms cool step was used to cool the ion/ion reaction product ions in Q0 before transmitting the product ions into the Q2 quadrupole where they were cooled again for 50 ms, transferred to Q3 (4.6×10^{-5} Torr) for 80 ms, cooled in Q3 for 50 ms and subjected to MSAE for mass analysis.

The Q0 quadrupole of the QTRAP was also used for positive-to-negative charge inversion of bradykinin using the PAMAM generation 1.5 dendrimer as the charge inversion reagent.

The positive to negative charge inversion reaction sequence involved injecting the PAMAM dendrimer anions into the Q0 quadrupole for 300 ms and storing them there by applying −22 V DC to the lens between Q0 and Q1. After cooling the PAMAM dendrimer ions in Q0 for 20 ms, the positive bradykinin ions were transmitted through the Q0 quadrupole for 1000 ms so that bradykinin +1/+2 ions were charge inverted to bradykinin −1. The positive analyte injection time for the transmission mode ion/ion reaction step can range from 50 ms to 1000 ms and is dependent upon the concentration of the analyte species being electrosprayed, its electrospray response, as well as the instrumental tuning parameters that affect ion transmission through the interface. Bradykinin anions formed via charge inversion as well as charge reduced dendrimer anions were then transferred to the Q3 quadrupole for 50 ms, where they were cooled for 50 ms before a mass spectrum was generated via MSAE.

Sequential charge inversion of bradykinin ions from positive to negative and back to positive using the Q0 array for the first charge inversion reaction and the Q2 array for the second reaction began with injection (50 ms) and cooling of the +9 charge state of the DAB generation 5 dendrimer in the Q2 collision cell (50 ms). Isolation of the DAB +9 charge state was performed by operating the Q1 quadrupole in mass resolving mode as the dendrimer ions were passed through Q1. Generation 1.5 PAMAM dendrimer anions were then injected into the Q0 quadrupole for 200 ms and cooled there (50 ms) by application of a −22 V repelling voltage to the lens between Q0 and Q1. Positive bradykinin ions were then injected into the Q0 quadrupole for 100 ms where some reacted with the PAMAM dendrimer ions and were converted to anions. The anions in Q0 were cooled for 50 ms before being transferred (80 ms) through the Q1 quadrupole, where bradykinin −1 was isolated from the population of charge-reduced PAMAM dendrimer ions, and into the Q2 quadrupole where the second ion/ion reaction occurred. When the isolated bradykinin −1 ions entered the Q2 quadrupole they reacted with the stored +9 DAB dendrimer ions and bradykinin was charge inverted from −1 to +1/+2. The positive product ions were cooled in Q2 for 50 ms and then were transferred to Q3 (80 ms) where they were again cooled for 50 ms before being subjected to MSAE for mass analysis.

Sequential charge inversion experiments performed solely in the Q2 collision cell began with ionization of the PAMAM dendrimer (300 ms) and transfer of the ions into the Q2 collision cell. The PAMAM dendrimer −6 charge state was isolated via operation of the Q1 quadrupole in mass resolving mode and the PAMAM dendrimer was cooled for 30 ms in Q2 with trapping DC. Bradykinin +1, which was also isolated via the Q1 quadrupole, was transferred through the instrument (300 ms) and into the Q2 quadrupole where it was charge inverted to −1 by the PAMAM dendrimer. The charge reduced PAMAM dendrimer anions and bradykinin −1 ions were cooled for 50 ms and transferred to Q3 for 80 ms where bradykinin −1 was isolated (10 ms) from the PAMAM dendrimer by operating the Q3 quadrupole in RF/DC mode. After isolating the bradykinin −1 ion, the +9 charge state of DAB generation 5 dendrimer was transferred (100 ms) into the Q2 quadrupole while storing negative bradykinin in the Q3 quadrupole. A 500 ms transfer step was used to transfer the bradykinin −1 ions into the Q2 quadrupole where they were charge inverted from −1 to +1/+2 ions via an ion/ion reaction with the DAB dendrimer cations. The charge inverted bradykinin ions and charge reduced DAB dendrimer ions were cooled in Q2 for 200 ms. A 200 ms cool step was necessary to remove all the untransferred bradykinin −1 ions from the Q3 quadrupole by application of attractive positive DC voltages to the end lenses and DC offset of the Q3 quadrupole. The product ions were then transferred to Q3 (80 ms) and cooled for 50 ms before being mass analyzed by MSAE. The double charge inversion experiments that used only the Q2 collision cell required roughly 700 ms more experimental time than the double charge inversion experiment that used both the Q0 and the Q2 quadrupoles. Most of the excess time resulted from the 500 ms step in which the bradykinin −1 ions were transferred from the Q3 to the Q2 quadrupole. Another 200 ms of experimental

time was used to remove the un-transferred bradykinin −1 ions from the Q3 quadrupole. It is necessary to eliminate these ions from Q3 before transferring the positive product ions into the Q3 quadrupole for mass analysis so that the negative and positive ions do not interact during the mass analysis step. These considerations would not apply if ion isolation in Q2 could be performed, which would obviate transfer into Q3 for ion isolation and subsequent transfer back to Q2. However, the Q2 collision cells in the instruments used here were not capable of performing ion isolation with adequate resolution for these purposes.

Transmission Mode Proton Transfer Reaction Sequence

For transmission mode ion/ion proton transfer reaction experiments in the Q0 cell of a QTRAP instrument, with and without ion parking, the high-voltage power supply for the nanospray source was pulsed on for 50 ms to generate positive protein ions, which were admitted into the Q0 quadrupole where they were collected by applying +22 V on the lens between Q0 and Q1. The protein ions were cooled in Q0 at a pressure of ~10 mTorr of nitrogen, for 50 ms, during which time the high voltage on the first emitter was turned off. After the cooling step, the power supply connected to the second nano-ESI emitter was triggered on for 150 ms to generate negative PFO reagent ions, which were transmitted through the Q0 quadrupole where they could react with the protein ions. The DC potentials, applied to the curtain plate and orifice, were adjusted during the previous cool step for the protein ions to allow the opposite polarity PFO ions to enter Q0 while continuing to trap the protein ions. After the transmission of reagent PFO ions through the Q0 quadrupole, the charge reduced protein ions were transmitted (100 ms) into Q3 (4.6×10^{-5} Torr) where they were cooled for 50 ms before being subjected to MSAE. When ion parking was used to concentrate a desired protein charge state during the ion/ion reaction within the Q0 array, a dipolar AC frequency was applied to one pair of rods in the Q0 rod set while the PFO anions were being transmitted through the Q0 quadrupole.

The experimental sequence for transmission mode proton transfer in the Q0 quadrupole of the QSTAR was very similar to that performed in the QTRAP. In the QSTAR experiment, a mixture of six proteins was subjected to nano-ESI for 300 ms during which time the cations were accumulated in Q0. Then, PFO anions were transmitted into the Q0 quadrupole for 100 to 700 ms to react with cations derived from the protein mixture and then the cationic product ions were cooled for 50 ms. The PFO anion injection time is determined by the PFO anion abundance level, the number of protein cations in Q0 and the desired extent to which charge state reduction is driven. A sine-wave was applied in dipolar fashion to a pair of opposing rods in Q0 to effect ion parking[14,15] during the PFO injection step to concentrate the desired protein charge states. In the case of high amplitude low frequency (HALF) parallel ion parking[15] of the entire six protein mixture, the product ions were cooled for 50 ms before being analyzed by TOF. The last experiment with the protein mixture involved single frequency on-resonance (SFOR) ion parking[14] of the +9 charge state of bovine ferri-cytochrome *c*. All residual cations, including the +9 cytochrome *c* ions, were transferred from Q0 to Q2 (80 ms) while using the Q1 quadrupole in resolving mode to transmit only the +9 charge state. During transfer into Q2, beam type CID was performed on the +9 charge state by increasing the relative voltage difference between the Q0 and Q2 quadrupole DC offsets to 65 V, resulting in a nominal injection energy of 585 eV. After the accumulation of cations in Q2, a second ion/ion reaction was performed in Q2 (100 ms injection of PFO anions) to charge reduce both the residual precursor ions and the product ions to predominantly the +1 charge state. This second ion/ion reaction was performed in mutual storage mode via the application of auxiliary RF (250 kHz, 500 $V_{p\text{-}p}$) to the end lenses of the Q2 quadrupole for 100 ms. After the charge reduced product ions were collisionally cooled for 30 ms, they were sent to the TOF analyser for mass analysis.

RESULTS AND DISCUSSION

Transmission Mode Charge Inversion

Charge inversion of bradykinin from negative to positive and from positive to negative has been performed in the Q0 cell of a linear ion trap by storing the reagent ion and injecting the analyte into Q0. In the negative to positive charge inversion case, deprotonated bradykinin is charge inverted while being transmitted through a stored population of DAB generation 4 dendrimer cations (predominantly the +6 charge state) in the RF-only Q0 cell, as illustrated in Figure 1 (see the experimental section for details of the experiment). Furthermore, charge inversion of a mixture of doubly and singly protonated bradykinin to deprotonated bradykinin in the Q0 cell using PAMAM dendrimer anions (predominantly the −6 and −5 charge states) as reagents is shown in Figure 2. (Note that the distribution of peaks in the PAMAM dendrimer anions for a given charge state are not comparable in the pre- and post-ion/ion reaction data. For example, many of the anions in the −4 charge state in the post ion/ion data were generated from the −6 ions in the pre-ion/ion data.) Based on comparison of the data in Figure 1 and Figure 2 with previously published results from analogous charge inversion experiments in the Q2 collision cell of QTRAP instruments34, charge inversion in the RF-only Q0 cell and Q2 collision cell is of comparable efficiency. Charge inverting an analyte species has several potential advantages. It allows analyte interrogation in both polarities via CID, which can provide complementary structural information, while ionization need only take place in one polarity. In addition, peptides that do not contain basic amino acids have been shown to charge invert more efficiently from negative to positive than peptides without basic amino acids32. Thus, charge inversion might also be used to discriminate between peptides based on their amino acid composition. Performing a transmission mode charge inversion experiment in Q0 allows further interrogation of the analyte species in Q2 (collision cell) or Q3 (the linear ion trap) with the option of an intervening mass selection step in Q1. For example, charge inversion in Q0 with mass selection of the charge inversion product of interest via Q1, followed by beam-type CID in Q2 is a relatively straightforward process. In this case, the mass selection and CID would essentially take place in parallel. A directly comparable experiment in which Q2 is the only ion/ion reaction region would entail charge inversion in Q2 with a transfer step to another quadrupole array for mass selection and subsequent injection back into Q2.

Double charge inversion of an analyte species via a transmission mode experiment is one example of how the use of Q0 for ion/ion reactions can increase the functionality of a hybrid linear ion trap by providing a novel means to perform two sequential ion/ion reactions. Experiments leading to the sequential charge inversion of the model analyte bradykinin were previously performed in both a 3D trap16 and a 2D ion trap35 (the Q2 collision cell) via mutual storage, the latter experiment requiring the application of auxiliary RF to the end lenses of the LIT. In both previous experiments, the bradykinin analyte was sequentially reacted with the PAMAM and the DAB dendrimer reagents within the same reaction volume. In both cases, multiple ion accumulation, ion isolation, and mutual ion storage steps were required to execute the experiment. In the case of the 2D trap, ion isolation of the intermediate product was accomplished by transferring the ions back and forth between Q1 and Q2, which increased the overall experimental time frame and reduced the duty cycle.

The use of Q0 as a reaction vessel for the first ion/ion reaction as well as the use of transmission mode ion/ion reactions makes it possible to reduce the overall time associated with a double charge inversion experiment. Figure 3 summarizes the double charge inversion of bradykinin (+1/+2 to −1 to +1/+2 performed on the 4000 QTRAP) and demonstrates use of both the Q0 quadrupole and the Q2 quadrupole as reaction vessels. Comparison of the double charge inversion of bradykinin performed only in the Q2 collision cell (data not shown) with the double charge inversion of bradykinin using both Q0 and Q2

showed that the use of Q0 for the first charge inversion ion/ion reaction reduced the overall time by 380 ms relative to the Q2-only experiment and eliminated several experimental steps associated with ion isolation and transfer.

Transmission Mode Proton Transfer Ion/Ion Reactions with Ion Parking

Proton transfer charge reduction of insulin via ion/ion reactions with PFO has been performed in the RF-only Q0 cell, both with and without ion parking. Charge reduction of a population of insulin cations, shown in Figure 4a, predominantly produces doubly charged insulin (see Figure 4b) in the displayed product ion spectrum. (Note that, based on the Z2 dependence of ion/ion reaction kinetics8, 36 and the low abundance of the +3 ions, it is likely that +1 insulin ions were produced in comparable abundance to the +2 ions. However, the +1 ions are not present in the Figure 4a because they fall outside the *m/z* range accessed by the MSAE conditions used here.) The application of an auxiliary AC frequency (32.633 kHz, 4 V_{p-p}) to an opposing pair of the Q0 rods during the transmission of the PFO anions through the stored insulin ion population, under otherwise identical conditions for generating the data of Figure 4b, gave rise to the data in Figure 4c. The selected frequency matched that of the fundamental secular frequency of the +4 insulin ion thereby accelerating ions of this charge state in one of the radial dimensions. In so doing, the overlap of the +4 ions with the transmitted PFO anions was reduced and the relative velocity of the oppositely charged ions was increased, thereby reducing the ion/ion reaction cross-section. The net result is the reduction of the rate for the ion/ion reaction of the +4 insulin ions. Under this condition, the charge reduction of the +5 and +6 ions is essentially stopped at the +4 charge state. The use of Q0 as a reaction cell, which imposes *m/z*-dependent frequencies of motion to the ions, adds a useful degree of control over the extent of reaction that would otherwise be absent if the reactions were conducted, for example, in the absence of an oscillating quadrupolar field.

Ion parking can also be used to inhibit the reactions of ions over a range of mass-to-charge values, provided that a means for broad-band ion acceleration is available. One such means is to simply use a relatively high amplitude single frequency that is lower than the secular frequencies of the ions to be parked15. (As the ion charge is reduced, the ion frequencies of motion in the ion trap are also reduced. Hence, it is necessary that the ion parking frequency be lower than the initial secular frequencies of the analyte ions so that the analyte ions move in the direction of a resonance condition with the applied frequency as the charge states change.) Off-resonance power absorption by ions of higher frequencies can lead to a deceleration of the ion/ion reaction rates for the same reasons that a single on-resonance frequency of low amplitude can inhibit reaction. The main difference is that the specificity of ion parking is lower with the higher amplitude condition. The latter approach has been referred to as high amplitude low frequency (HALF) parallel ion parking37. The inset in Figure 5a shows the positive nano-ESI mass spectrum of a mixture of six proteins (bovine cytochrome *c*, equine cytochrome *c*, insulin, ubiquitin, myoglobin and lysozyme), in which the most abundant ions are singly charged contaminant ions. The other two spectra shown in Figure 5 compare transmission mode ion/ion reaction results over a common *m/z* range for the mixture of ions in the inset after anions derived from PFO were transmitted through the stored cation population in Q0 without (Figure 5a) and with (Figure 5b) parallel ion parking. In the absence of ion parking, charge reduction of the proteins in this mixture via ion/ion reactions with PFO reduces the proteins to charge states of ≤ +2. For all the proteins except insulin and ubiquitin, the charge reduced protein product ions fall outside the *m/z* range shown in this comparison (data not shown). The results of Figure 5a demonstrate that it is straightforward to reduce protein charge states to low values in Q0. However, it may be desirable to limit the extent of charge reduction without having to carefully control the abundances of the cations and anions. Parallel ion parking provides a means to do so for

multiple analytes simultaneously. Figure 5b shows the results obtained using conditions identical to those used to generate Figure 5a with the exception of the application of a 12 kHz, 7 V_{p-p} frequency to a pair of opposing rods of Q0 during the ion/ion reaction period. As is evident from Figure 5b, ions from all six proteins in the mixture are clearly apparent and most of the signal from each protein is concentrated into two or three dominant charge states. These results demonstrate that parallel ion parking can be effected in Q0. No clear differences in performance for parallel ion parking in Q0 versus parallel ion parking in Q2 (data not shown) have been noted.

Ion parking in Q0, either via the more highly selective single frequency low-amplitude approach or via a broad-band parallel ion parking approach, can be used to generate and concentrate ions from high charge states to lower charge states for subsequent activation in Q2. The mass selection quadrupole, Q1, can be used to select a precursor ion from Q0 for beam-type collisional activation in Q2 in the course of ion transmission between Q1 and Q2. This can provide significant time savings relative to the use of Q2 for all ion processing (i.e., ion parking and beam-type collisional activation), which, in the case of the exclusive use of Q2, can involve a more complex experimental sequence with one or more additional ion transfer steps. An example of the use of ion/ion reactions in both Q0 and Q2 for the tandem mass spectrometry of an intact protein ion is illustrated in Figure 6. Figure 6a and 6b compare isolated bovine ferri-cytochrome *c* +9 precursors ions from the mixture of protein ions depicted in the inset of Figure 5 without ion/ion reactions in Q0 (Figure 6a) and after the use of ion/ion reactions in Q0 in conjunction with single-frequency ion parking (Figure 6b). In this particular instance, the solution conditions already gave rise to some +9 bovine ferri-cytochrome *c* signal in the nano-ESI mass spectrum. Ion/ion reactions with ion parking increased the +9 cytochrome *c* precursor ion signal 3–4 fold (compare Figures 6a and 6b). The precursor ions concentrated via ion parking in Q0 were then mass selected via Q1 and subjected to beam-type collisional activation by injecting the ions into Q2 at a kinetic energy of 585 eV. The end lenses of Q2 were adjusted to trap the injected precursor ions along with the CID products generated via collisions with the nitrogen gas in the collision cell. The residual precursor ions as well as the CID products were then subjected to ion/ion proton transfer reactions with PFO anions, in this case via the mutual storage of both ion polarities in Q2, to reduce the charge states largely to +1 before the cations were subjected to TOF analysis. The results are summarized in Figure 6c–e, which provide three segments of the product ion spectrum that collectively summarize the product ions over the *m/z* range of 350–12,500. Evidence for roughly 60% of the possible amide bond cleavages is observed. As expected, beam-type CID, which involves higher dissociation rates than does ion trap CID and therefore tends to sample ions of higher internal energies, yields more product ions than does ion trap CID38 and, as a consequence, greater sequence coverage. (Less than 50% sequence coverage was obtained via ion trap CID for charge states +6 to +15 of bovine ferri-cytochrome *c*.) The higher energy deposition is also reflected in the production of a large number of “a” and “a*” ions as well as from product ions that are probably the result of secondary fragmentation (e.g. the relatively abundant ions that are labeled with an asterisk in Figures 6c–e). The ability to effect precursor ion charge manipulation in Q0, rather than Q2, is particularly useful for the interrogation of whole protein ions via beam-type CID. Otherwise, it would be necessary to remove the precursor ions from Q2 for re-injection into Q2 to effect beam-type CID. Such a procedure would require additional transfer steps that would add to the overall time of the experiment, reduce the duty cycle, and provide greater opportunities for transmission losses upon ion transfer from one quadrupole array to another.

Conclusions

Transmission mode ion/ion reactions within the RF-only quadrupole of a hybrid tandem mass spectrometer, which is ordinarily used to transmit ions from an atmosphere/vacuum

interface to a mass filter, can add functionality relative to instruments that restrict ion/ion reactions to a collision cell between mass analysis elements. Advantages are realized when all ions pass through the instrument along the same ion path and in the same direction (i.e., when all ions pass through the RF-only quadrupole prior to entering the first mass analysis element in the tandem mass spectrometer, as is the case when a common vacuum/atmosphere interface is used for both ion polarities). When this is the case, an ion/ion reaction in Q0 can reduce the number of ion transfer steps and overall analysis time in experiments that involve two or more ion transformation steps (e.g. two ion/ion reactions, an ion/ion reaction followed by beam-type CID, etc.). In this work, transmission mode ion/ion reactions have been demonstrated in the Q0 RF-only ion transmission quadrupoles of hybrid triple quadrupole/linear ion trap and hybrid quadrupole/time-of-flight tandem mass spectrometers. The results obtained from these experiments suggest that transmission mode ion/ion reactions within the Q0 quadrupole are as efficient as ion/ion reactions within the Q2 collision cell of the instrument. The use of the Q0 quadrupole for preparatory ion/ion reactions can enhance the overall functionality of hybrid tandem mass spectrometers, as shown via both proton transfer charge inversion and charge reduction experiments. Charge inverting the analyte species within the Q0 quadrupole, as demonstrated in this work, is a way to separate the ionization polarity from the analysis polarity of a peptide. An important consequence of the use of a quadrupole array as the ion transmission device is the fact that the ions have *m/z*-dependent frequencies of motion. If a supplementary low RF voltage can be added to a pair of opposing rods in the array, the ion parking technique can be applied in Q0. This allows for either a selective inhibition of ion/ion reaction rates in Q0, via low amplitude on-resonance excitation, or broad-band inhibition of reaction rates, via, for example, high amplitude low-frequency excitation, for either single ion parking or parallel ion parking, respectively, in Q0. These capabilities are useful additions to the growing array of ion/ion reaction experiments that can be conducted with hybrid tandem mass spectrometers.

Acknowledgments

This research was supported by the National Institutes of Health under Grant GM 45372 and by MDS Sciex, a discovery partner of the Department of Chemistry at Purdue University.

References

1. Fenn JB, Mann M, Meng CK, Wong SF, Whitehouse CM. Science. 1989; 246:64. [PubMed: 2675315]
2. Loo RRO, Udseth HR, Smith RD. J. Phys. Chem. 1991; 95:6412.
3. Loo RRO, Smith RD. J. Mass Spectrom. 1995; 30:339.
4. Herron WJ, Goeringer DE, Mcluckey SA. J. Am. Soc. Mass Spectrom. 1995; 6:529.
5. Stephenson JL Jr, McLuckey SA. J. Am. Chem. Soc. 1996; 118:7390.
6. Scalf M, Westphall MS, Krause J, Kaufman SL, Smith LM. Science. 1999; 283:194. [PubMed: 9880246]
7. Ebeling DD, Westphall MS, Scalf M, Smith LM. Anal. Chem. 2000; 72:5158. [PubMed: 11080858]
8. McLuckey SA, Stephenson JL Jr, Asano KG. Anal. Chem. 1998; 70:1198. [PubMed: 9530009]
9. McLuckey SA, Wu J, Bundy JL, Stephenson JL Jr, Hurst GB. Anal. Chem. 2002; 74:976. [PubMed: 11925000]
10. Stephenson JL Jr, McLuckey SA. Anal. Chem. 1998; 70:3533. [PubMed: 9737205]
11. Schaaff TG, Cargile BJ, Stephenson JL, McLuckey SA. Anal. Chem. 2000; 72:899. [PubMed: 10739190]
12. Hogan JM, McLuckey SA. J. Mass Spectrom. 2003; 38:245. [PubMed: 12644985]
13. Amunugama R, Hogan JM, Newton KA, McLuckey SA. Anal. Chem. 2004; 76:720. [PubMed: 14750868]

14. McLuckey SA, Reid GE, Wells JM. Anal. Chem. 2002; 74:336. [PubMed: 11811406]
15. Chrisman PA, Pitteri SJ, McLuckey SA. Anal. Chem. 2005; 77:3411. [PubMed: 15889938]
16. He M, McLuckey SA. J. Am. Chem. Soc. 2003; 125:7756. [PubMed: 12822966]
17. He M, Emory JF, McLuckey SA. Anal. Chem. 2005; 77:3173. [PubMed: 15889906]
18. Gunawardena HP, Emory JF, McLuckey SA. Anal. Chem. 2006; 78:3788. [PubMed: 16737238]
19. Herron WJ, Goeringer DE, Mcluckey SA. J. Am. Chem. Soc. 1995; 117:11555.
20. Schwartz JC, Senko MW, Syka JEP. J. Am. Soc. Mass Spectrom. 2002; 13:659. [PubMed: 12056566]
21. Hager JW. Rapid Commun. Mass Spectrom. 2002; 16:512.
22. Syka JEP, Coon JJ, Schroeder MJ, Shabanowitz J, Hunt DF. Proc. Natl. Acad. Sci. 2004; 101:9528. [PubMed: 15210983]
23. Wu J, Hager JW, Xia Y, Londry FA, McLuckey SA. Anal. Chem. 2004; 76:5006. [PubMed: 15373435]
24. Xia Y, Chrisman PA, Erickson DE, Liu J, Liang X, Londry FA, Yang MJ, McLuckey SA. Anal. Chem. 2006; 78:4146. [PubMed: 16771545]
25. Kaplan DA, Hartmer R, Speir JP, Stoermer C, Gumerov D, Easterling ML, Brekenfeld A, Kim T, Laukien F, Park MA. Rapid Commun. Mass Spectrom. 2008; 22:271. [PubMed: 18181247]
26. McAlister GC, Berggren WT, Griep-Raming J, Horning S, Makarov A, Phanstiel D, Stafford G, Swaney DL, Syka JEP, Zabrouskov V, Coon JJJ. Proteome Res. 2008; 7:3127.
27. McAlister GC, Phanstiel D, Good DM, Berggren WT, Coon JJ. Anal. Chem. 2007; 79:3525. [PubMed: 17441688]
28. Xia Y, Wu J, McLuckey SA, Londry FA, Hager JW. J. Am. Soc. Mass Spectrom. 2005; 16:71. [PubMed: 15653365]
29. Liang XR, Hager JW, McLuckey SA. Anal. Chem. 2007; 79:3363. [PubMed: 17388568]
30. Liang XR, McLuckey SA. J. Am. Soc. Mass Spectrom. 2007; 18:882. [PubMed: 17349802]
31. Liang XR, Han HL, Xia Y, McLuckey SA. J. Am. Soc. Mass Spectrom. 2007; 18:369. [PubMed: 17101274]
32. Emory JF, McLuckey SA. J. Am. Soc. Mass Spectrom. 2008
33. Londry FA, Hager JW. J. Am. Soc. Mass Spectrom. 2003; 14:1130. [PubMed: 14530094]
34. Emory JF, McLuckey SA. Int. J. Mass Spectrom. 2008; 276:102.
35. Xia Y, Thomson BA, McLuckey SA. Anal. Chem. 2007; 79:8199. [PubMed: 17914865]
36. Wells JM, Chrisman PA, McLuckey SA. J. Am. Chem. Soc. 2003; 125:7238. [PubMed: 12797797]
37. Chrisman PA, Pitteri SJ, McLuckey SA. Anal. Chem. 2006; 78:310. [PubMed: 16383342]
38. Engel BJ, Pan P, Reid GE, Wells JM, McLuckey SA. Int. J. Mass Spectrom. 2002; 219:171.

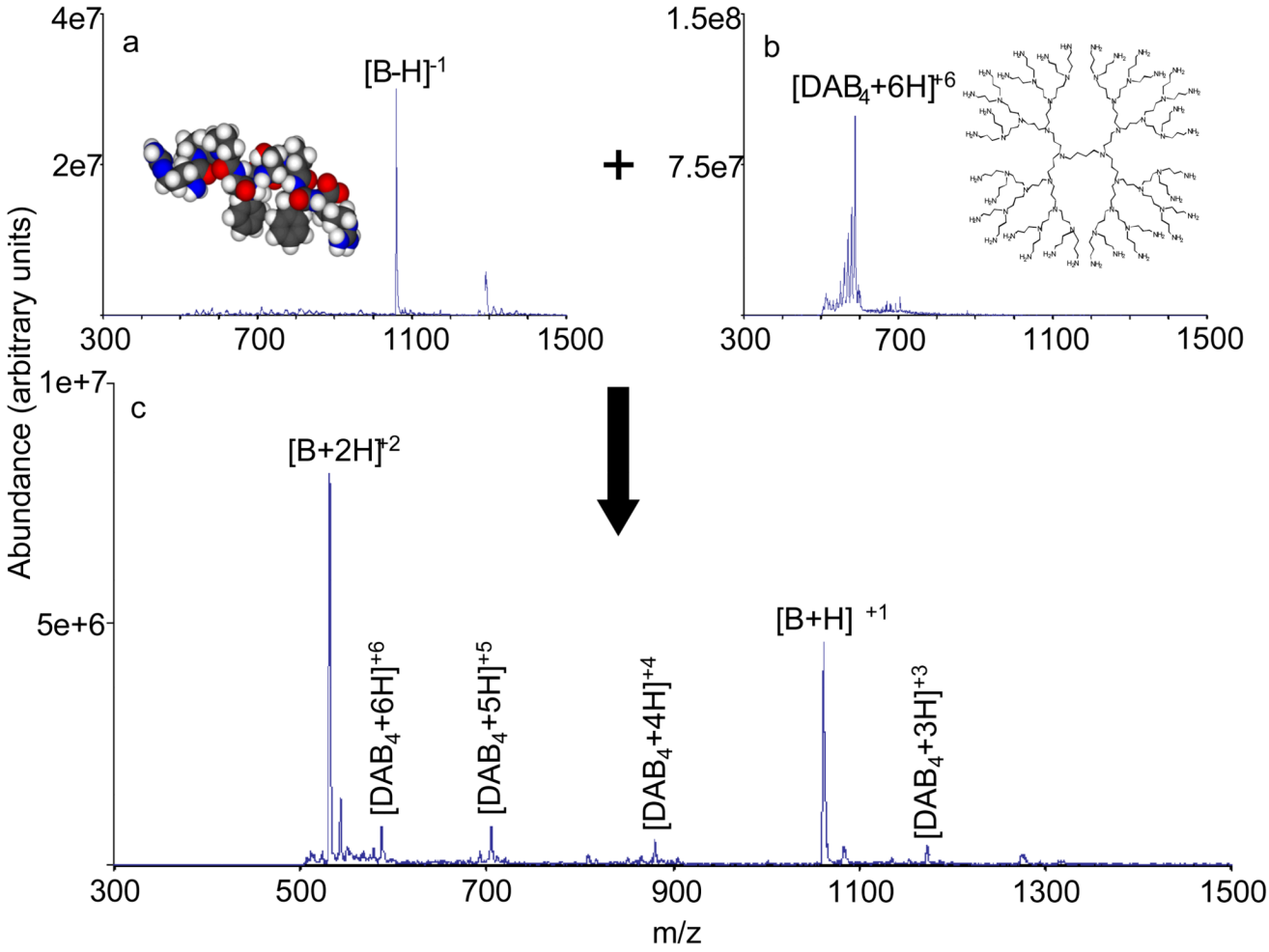

Figure 1.

Summary of a transmission mode charge inversion experiment in Q0 involving bradykinin −1 to bradykinin +2/+1. a.) Bradykinin −1 nano-ESI mass spectrum; b.) nano-ESI mass spectrum of DAB generation 4 dendrimer, predominantly the +6 charge state; and c.) product positive ion spectrum of the ion/ion reaction of the ions of “a” and “b” which shows the charge inverted bradykinin +2/+1 ions and charge reduced DAB dendrimer ions.

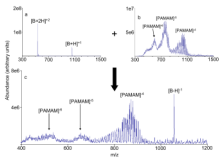

Figure 2.
Summary of a transmission mode experiment for positive to negative charge inversion of bradykinin. a.) Positive nano-ESI mass spectrum of bradykinin; b.) negative nano-ESI mass spectrum of PAMAM generation 1.5 dendrimer anions stored in Q0; and c.) the product ions of the charge inversion reaction resulting from interaction of the bradykinin cations and the PAMAM dendrimer anions.

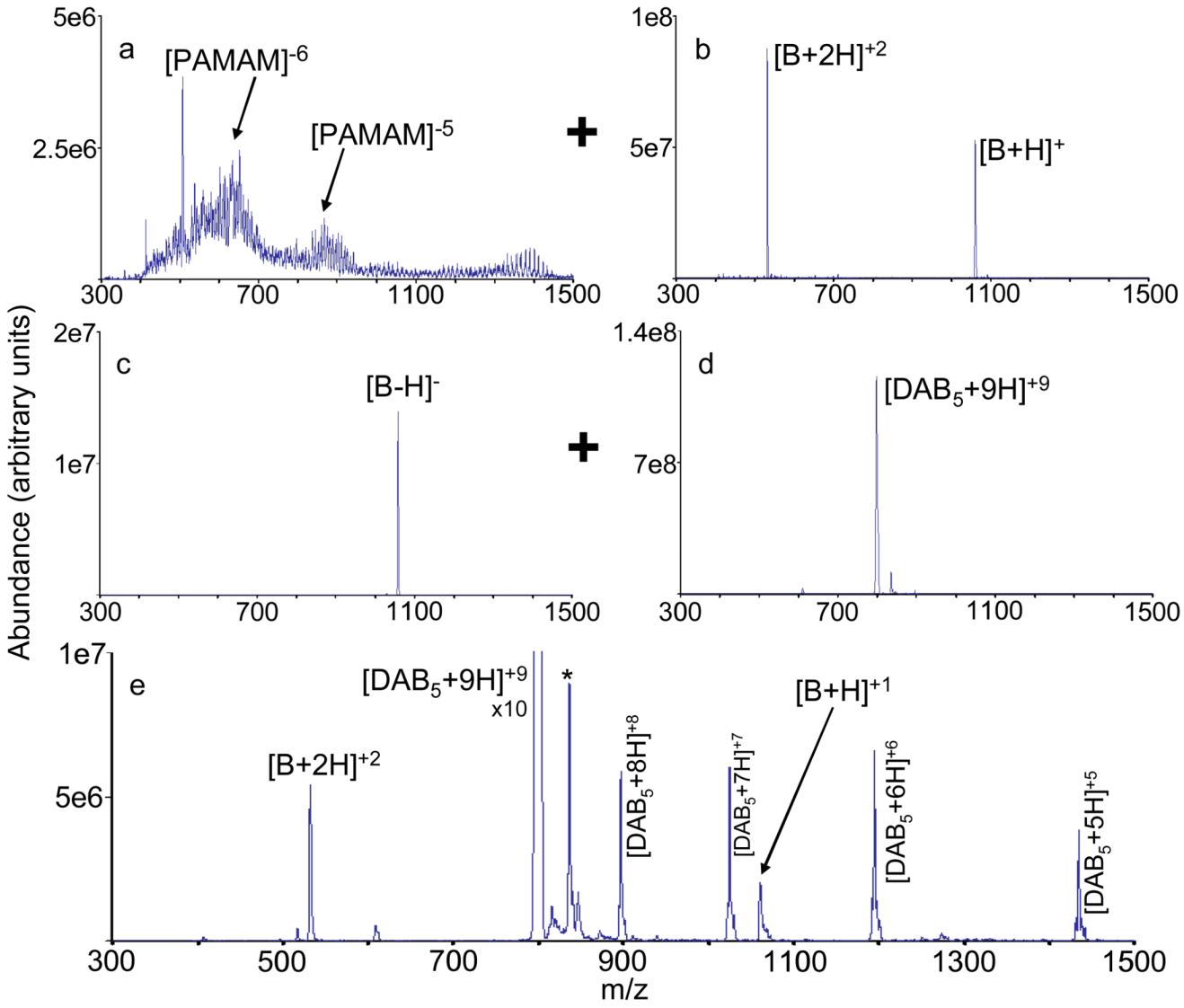

Figure 3.

a.) PAMAM dendrimer generation 1.5 anions used for positive to negative charge inversion of bradykinin +1/+2 in Q0; b.) bradykinin +1/+2 ions passed into Q0 for first ion/ion reaction; c.) Q1 isolated bradykinin −1 ions passed into Q2 for second charge inversion reaction; d.) isolated DAB generation 5 +9 ions previously stored in the Q2 collision cell; and e.) charge inversion of bradykinin −1 produced by reaction of ions in panels c. and d., giving double charge inversion of bradykinin. The asterisk represents an ion produced from DAB dendrimer isolation.

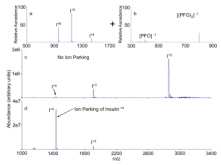

Figure 4.

a.) Insulin positive nano-ESI mass spectrum b.) PFO negative negative nano-ESI mass spectrum. c.) Post-ion/ion reaction data for the insulin ions stored in Q0 with transmission of PFO anions. d.) Single frequency on resonance (SFOR) ion parking of the insulin +4 charge state during the charge reduction of insulin in Q0 via ion/ion reaction with PFO anions.

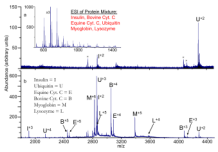

Figure 5.

a.) Post-ion/ion reaction mass spectrum following the reaction of cations formed from a mixture of six proteins (see inset for pre-ion/ion reaction mass spectrum of the protein mixture) with anions derived from PFO in Q0. b.) Post-ion/ion product ion spectrum of the protein mixture obtained under the same conditions as for 5a but with the application of a 12 kHz, 7 V_{p-p} frequency. The asterisks indicate noise peaks.

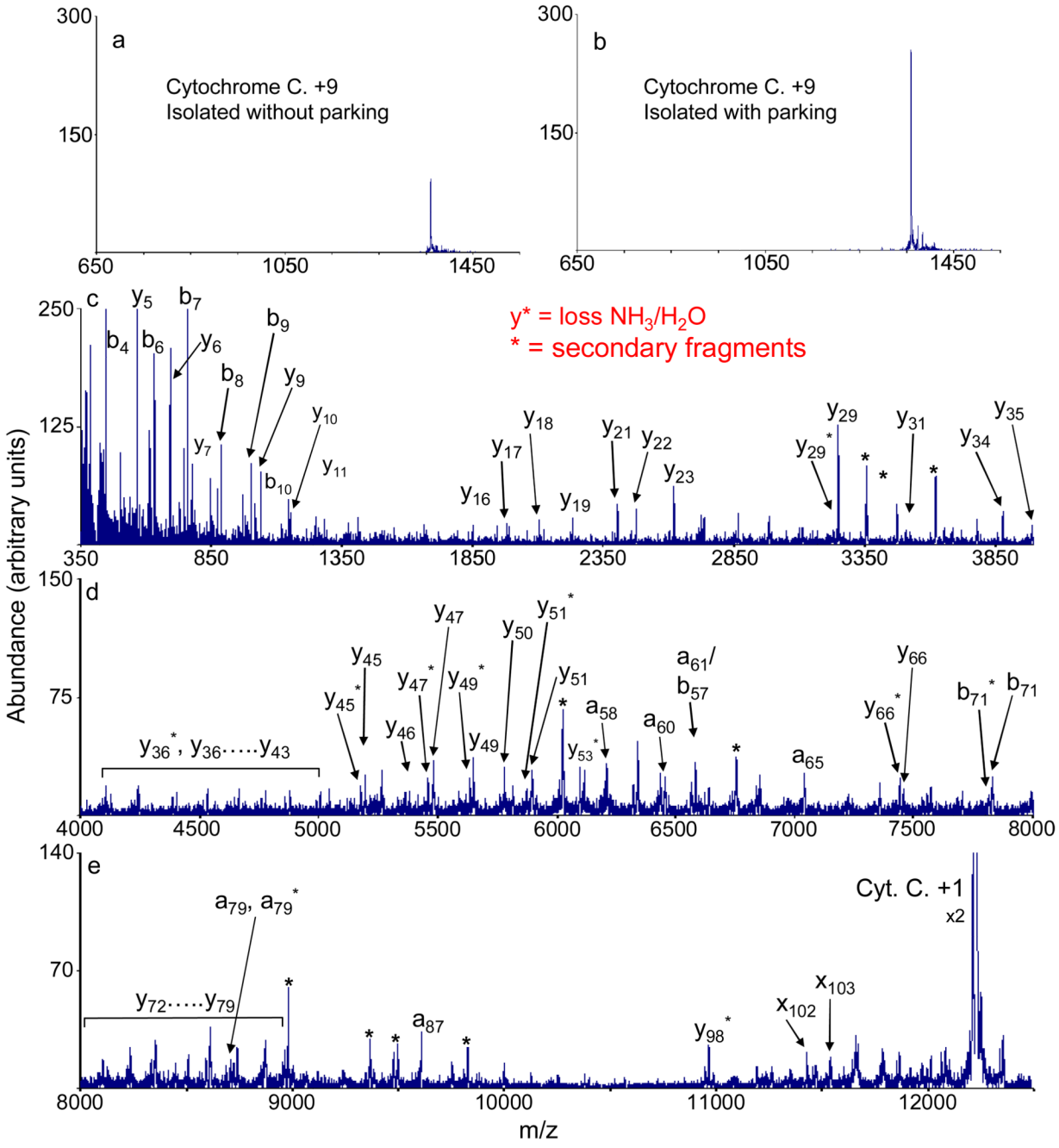

Figure 6.

(a) Isolated +9 charge state of bovine ferri-cytochrome *c* generated directly from nano-ESI of the six component protein mixture. (b) Isolated +9 charge state of bovine ferri-cytochrome *c* following a transmission mode ion parking (27.8 kHz, 4 V_{p-p}) procedure in the Q0 quadrupole array (27.8 kHz, 4 V_{p-p}). The final three panels (c, d and e) show the charge reduced CID spectrum of +9 cytochrome c.